^{3}He$(\gamma,2p)n$ reaction*

B. F. Gibson
Theoretical Division, Los Alamos Scientific Laboratory, University of California, Los Alamos, New Mexico 87545

D. R. Lehman
Department of Physics, The George Washington University, Washington D. C. 20052

(Received 4 October 1976)

Cross sections for the ^{3}He$(\gamma,2p)n$ coincidence reaction are calculated in the energy range $15 \leq E_\gamma \leq 50$ MeV for the coplanar geometry. The calculation is performed within the context of exact three-body theory where the two-nucleon interactions are represented by s-wave spin-dependent separable potentials fitted to low-energy nucleon-nucleon scattering data. The Coulomb force between the protons is neglected. The cross section is found to be most sensitive to the parametrization of the singlet interaction in the final state when two nucleons exit in close proximity.

[NUCLEAR REACTIONS Photodisintegration of ^{3}He; exact three-body calculation; separable potentials; coincidence cross sections.]

I. INTRODUCTION

Coincidence experiments involving an electromagnetic probe of the nucleus have been advanced as providing a sensitive test of the ground-state wave function.[1-4] In particular, it was shown that the ^{3}He$(e,e'd)p$ reaction could be used to distinguish among various available *ad hoc* assumptions for the radial dependence of the three-body ground state.[1,2] In view of the possibility of performing coincidence experiments such as ^{3}He$(\gamma,2p)n$ at high current accelerators like Bates,[5] we wish to examine briefly the question of what information might be reliably extracted from these reactions. Specifically, we wish to investigate the dependence of the cross section upon the ground-state-model assumption, the sensitivity of the cross section to the rescattering of the three nucleons in the final state, and the photon energy range most easily analyzed. The first of these questions is motivated by the 15% difference in the total cross section estimates obtained for the trinucleon models constructed in Refs. 6 and 7 and the possibility that the difference might be amplified in the coincidence geometry. The second question concerns whether the ground-state differences can be discerned when rescattering effects are large, as well as whether the rescattering of a single pair of nucleons will completely dominate in a particular geometry—the same point to which the last question pertains.

We perform this investigation utilizing the mathematically simplifying assumption of a separable potential representation of the N-N interaction. The parameters of the s-wave spin-dependent rank-one potential are determined from the N-N singlet and triplet scattering length and effective range. The singlet phase shifts are reasonably well reproduced below 100 MeV; the triplet phase shifts are not so well represented, since we neglect the tensor component of the triplet force. Except for use of the model in Ref. 6, the initial as well as the final states are determined from the same interactions. We neglect the Coulomb interaction of the two protons, although we do consider the effect of including the modification of the p-p strong interaction in the final state due to the presence of the Coulomb force. Throughout this investigation, we restrict ourselves to the dominant $l=1$ electric-dipole transition. Our formalism is briefly reviewed in the following section, where we also develop the appropriate cross section expressions. Our numerical results and corresponding discussion are presented in Sec. III. Our conclusions are summarized in Sec. IV.

II. THEORETICAL REVIEW

The formulation of the theory of the three-body photodisintegration of ^{3}He and ^{3}H, which we utilize, is described in detail in Ref. 7. The amplitude for this process can be expressed as the sum of three terms

$$A_3(\alpha,n,\vec{p},\vec{k}) = \langle \Phi^0_{\alpha n \vec{p}\vec{k}} | H' | \psi_B \rangle - \sum_{\beta=1}^{3} \langle \Phi^0_{\alpha n \vec{p}\vec{k}} | T_\beta(z) G_0(z) H' | \psi_B \rangle + \sum_{\beta,\gamma=1}^{3} \langle \Phi^0_{\alpha n \vec{p}\vec{k}} | T_\gamma(z) X_{\gamma\beta}(z) G_0(z) H' | \psi_B \rangle \quad (1)$$

with $z = E^{(3)}_{\alpha n} + i\eta$. Here $|\Phi^0_{\alpha n \vec{p}\vec{k}}\rangle$ describes the three-

body plane-wave final state of three nucleons; $\vec{p}_\alpha$ is the relative momentum of nucleon α with respect to the center of mass of particles β and γ; $\vec{k}_{\beta\gamma}$ is the relative momentum of nucleons β and γ; and n is an index labeling quantum numbers such as the spin and isospin. H' is the electromagnetic interaction, which is treated perturbatively; $T_\beta(z)$ is the two-body T operator; $G_0(z)$ is the resolvent operator $(H_0 - z)^{-1}$; and $X_{\gamma\beta}(z)$ is the transition operator connecting particle-plus-correlated-pair states. The three terms in Eq. (1)—designated the plane-wave Born term, the first rescattering term, and the term which sums all rescattering beyond the first—are depicted diagrammatically along with the integral equations for the transition operator $X_{\gamma\beta}$ in Fig. 1.

Restricting the perturbative Hamiltonian to the $E1$ transition, we have

$$H' = \tfrac{1}{2}\, e \sum_{i=1}^{3} (\hat{\epsilon}\cdot\vec{r}_i)\tau_3^i \,, \tag{2}$$

where $\vec{r}_i$ is the nucleon center-of-mass coordinate, $\hat{\epsilon}$ is the photon polarization unit vector, and τ_3^i is the third (z component) isospin Pauli matrix for nucleon i. H' operates on the ground state, which we take to be the dominant spatially symmetric component. The resulting amplitudes are of the form (S_{23} and I_{23} are the spin and isospin coupling of particles 2 and 3)

$$\mathfrak{M}_3^{S_{23}} = -(\tfrac{2}{3})^{1/2} M^{1/2}_{S_{23}1} + (\tfrac{1}{3})^{1/2} M^{3/2}_{S_{23}1} \tag{3}$$

for the $^3\mathrm{He}(\gamma, 2p)n$ reaction and of the form

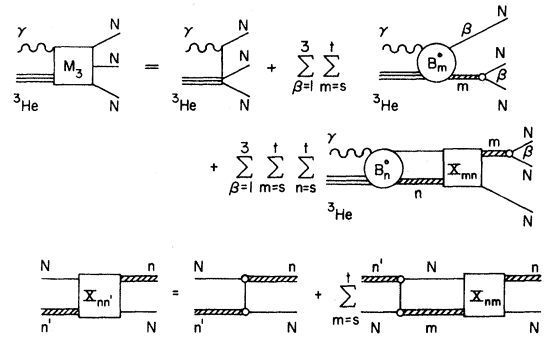

FIG. 1. Diagrammatic representation of the calculation of the three-body photodisintegration amplitude. The wavy line represents the disintegration mechanism (i.e., in the case of photodisintegration a photon), the triple lines the trinucleon ground state, and the cross-hatched double lines a particular correlated pair plus nucleon (N) being off shell. The upper part of the figure describes the amplitude M_3 as a sum of Born, first rescattering, and integral over the off-shell scattering amplitude X_{mn}; B_m^0 is the off-shell Born amplitude. The lower part of the figure describes the integral equation that determines the off-shell scattering amplitude $X_{nn'}$.

$$\mathfrak{M}_3^{S_{23}} = \frac{1}{\sqrt{2}}\,(M^{1/2}_{S_{23}0} + (\tfrac{1}{3})^{1/2} M^{1/2}_{S_{23}1} + (\tfrac{2}{3})^{1/2} M^{3/2}_{S_{23}1}) \tag{4}$$

for the $^3\mathrm{He}(\gamma, np)p$ reaction. The $M^I_{S_{23}I_{23}}$ can be expressed as a sum of three terms:

$$M^I_{S_{23}I_{23}} = C^I_{S_{23}I_{23}}(\vec{p},\vec{k}) + F^I_{S_{23}I_{23}}(z,\vec{p},\vec{k}) + S^I_{S_{23}I_{23}}(z,\vec{p},\vec{k}) \,, \tag{5}$$

where C is the plane-wave Born amplitude, F is the first rescattering amplitude, and S is the amplitude that sums the remaining terms. Because of a misprint in our tabulation of the plane-wave Born terms in Ref. 7, we repeat them here:

$$\begin{aligned}
C^{1/2}_{01} &= -\,e\frac{1}{\sqrt{6}}\,\hat{\epsilon}\cdot\vec{p}_{op}\,\psi^s_0(\vec{k},\vec{p}) \,,\\
C^{1/2}_{00} &= e\frac{1}{2\sqrt{2}}\,\hat{\epsilon}\cdot\vec{r}_{op}\psi^s_0(\vec{k},\vec{p}) \,,\\
C^{1/2}_{10} &= C^{1/2}_{01} \,,\\
C^{1/2}_{11} &= -\,C^{1/2}_{00} \,,\\
C^{3/2}_{01} &= -\sqrt{2}\,C^{1/2}_{01} \,,\\
C^{3/2}_{11} &= \sqrt{2}\,C^{1/2}_{11} \,.
\end{aligned} \tag{6}$$

The remainder of the terms are as given in Eq. (45) through Eq. (52) of Ref. 7.

As a function of the amplitudes $\mathfrak{M}_3^{S_{23}}$, the three-body coincidence cross section has the form

$$d\sigma = \frac{4\pi^2}{\hbar c}\,E_\gamma \sum_{S_{23}=0}^{1} \left|\mathfrak{M}_3^{S_{23}}\left(\frac{3p^2}{4m} + \frac{k^2}{m}\,,\vec{p},\vec{k}\right)\right|^2_{\text{pol. ave.}} \rho_f \,. \tag{7}$$

In the specific case of the $^3\mathrm{He}(\gamma, 2p)n$ cross section considered below, one is detecting both of the protons, and the identical particle problem is minimal. The appropriate density of states is given by[8]

$$\rho_f = 2m^2\,\frac{p_2^{\,2}p_3}{|2p_2 + \hat{p}_2\cdot(\vec{p}_3 - \vec{q})|}\,dE_3\,d\Omega_3\,d\Omega_2 \,, \tag{8}$$

where

$$\int d\Omega_2\,d\Omega_3 = \tfrac{1}{2}(4\pi)^2 \,.$$

The coplanar geometry implied in these expressions is defined in Fig. 2; $\vec{q}$ is the photon momentum. One notes that in addition to the usual relative momenta relations

$$\begin{aligned}
\vec{k} &= \tfrac{1}{2}(\vec{p}_2 - \vec{p}_3) \,,\\
\vec{p} &= \tfrac{2}{3}\vec{p}_1 - \tfrac{1}{3}(\vec{p}_2 + \vec{p}_3) \,,\\
\vec{k}\cdot\vec{p} &= -\tfrac{1}{2}(p_2^2 - p_3^2) + \tfrac{1}{3}\vec{q}\cdot(\vec{p}_2 - \vec{p}_3) \,,
\end{aligned} \tag{9}$$

one also needs for the polarization sum

$$(\hat{\epsilon}\cdot\hat{r}):\ |\hat{q}\times\hat{k}| = \frac{1}{2k}\left[p_2\cos\theta_2 - p_3\cos\theta_3\right],$$

$$(\hat{\epsilon}\cdot\hat{p}):\ |\hat{q}\times\hat{p}| = \frac{1}{p}\left[\tfrac{2}{3}p_1\cos\theta_1 - \tfrac{1}{3}(p_2\cos\theta_2 + p_3\cos\theta_3)\right], \quad (10)$$

$$(\hat{\epsilon}\cdot\hat{p})\,(\hat{\epsilon}\cdot\hat{r}):\ \cos\phi_{pk} = \vec{p}\cdot\vec{k}/|\vec{p}\cdot\vec{k}|\,.$$

III. NUMERICAL RESULTS

We consider the specific reaction ^{3}He(γ, 2p)n for the case of uncharged protons. We restrict our consideration to the energy range 15 MeV $\leq E_\gamma \leq$ 50 MeV, where the long-wave-length limit approximation for the dominant $E1$ operator is valid. For the coplanar geometry defined in Fig. 2, we consider equal proton opening angles ($\theta_2 = \theta_3$) of 5°, 10°, and 20°. The small opening angle exemplifies the situation in which the two protons exit "close" to one another and therefore have the opportunity to interact strongly. The large opening angle provides an example of what to expect when all of the nucleons are "far apart," so that no one-pair interaction should dominate.

In Figs. 3–6, we present results for the three opening angles noted above at energies of 15, 20, 30, and 50 MeV. The 15 MeV energy is near the peak in the total cross section, and the coincidence cross section is largest there for any given angular configuration. The coincidence cross section is a maximum at each energy for the 5° opening angle, where the enhancement due to the strong final-state p-p interaction is the largest. The peak in the cross section occurs at $E_2 \approx E_3$, where the relative p-p energy is a mimium. Near this peak, the

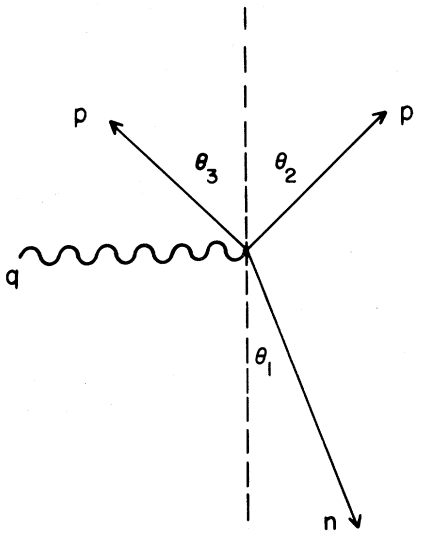

FIG. 2. Coplanar geometry for which the coincidence calculations were performed.

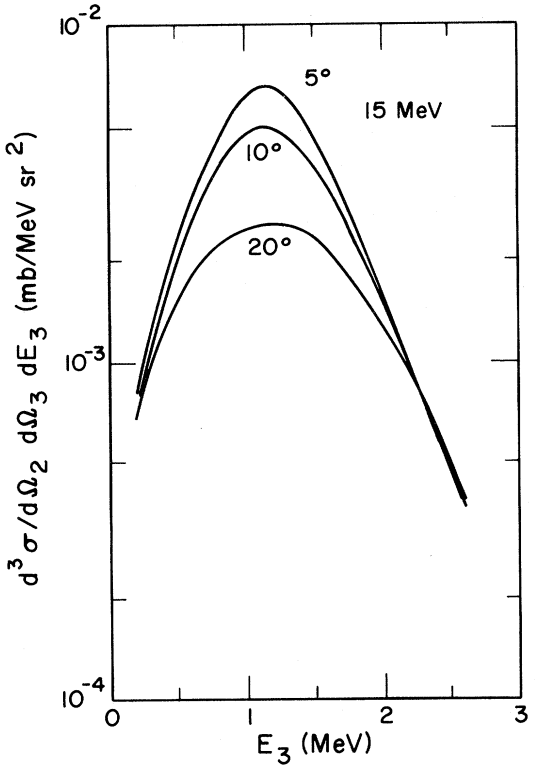

FIG. 3. Comparison of coincidence spectra at E_γ = 15 MeV for $\theta_2 = \theta_3$ as noted.

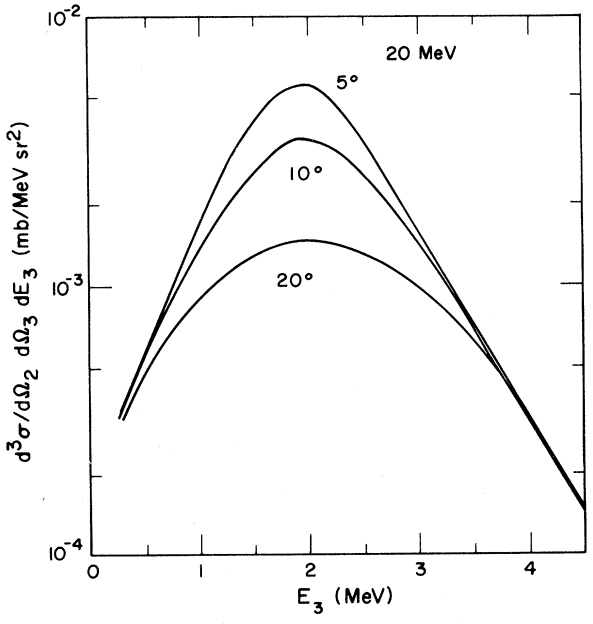

FIG. 4. Comparison of coincidence spectra at E_γ = 20 MeV for $\theta_2 = \theta_3$ as noted.

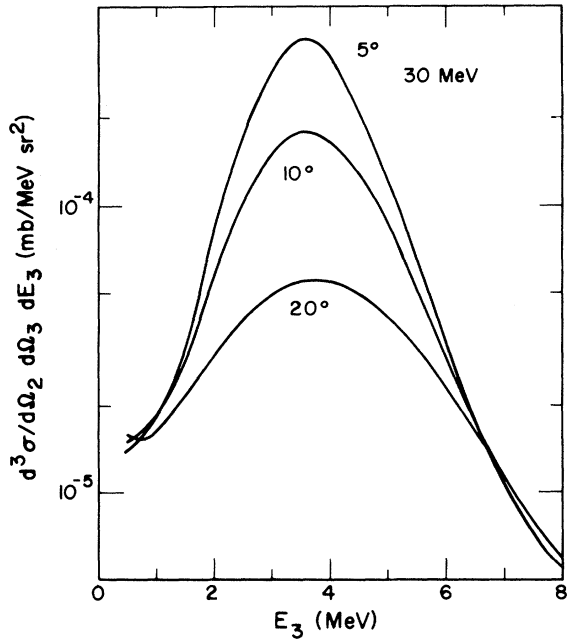

FIG. 5. Comparison of coincidence spectra at $E_\gamma = 30$ MeV for $\theta_2 = \theta_3$ as noted.

cross section varies rapidly as a function of opening angle, implying that precise angular resolution will be required in order to extract useful information. One may note the minima in the

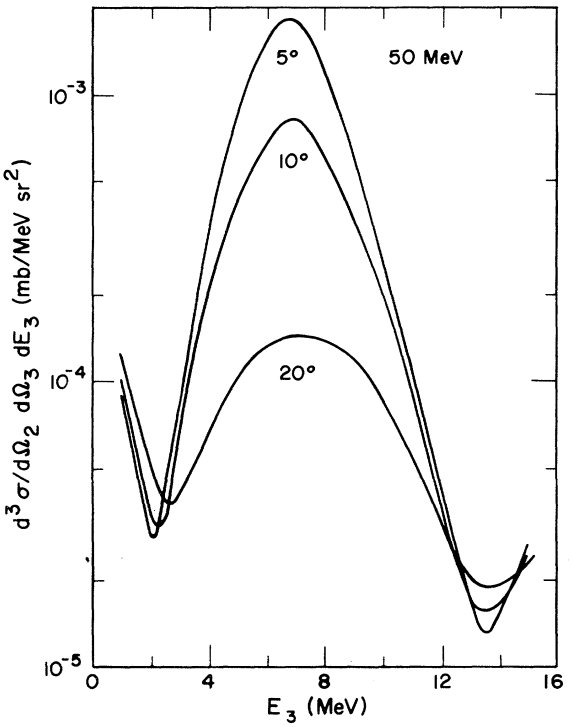

FIG. 6. Comparison of coincidence spectra at $E_\gamma = 50$ MeV for $\theta_2 = \theta_3$ as noted.

50 MeV results in Fig. 6. This is apparently a final-state rescattering effect, since the plane-wave Born calculation results in a curve which peaks near $E_3 = 2$ MeV and falls off monotonically as E_3 increases.

In Fig. 7, we address the question of model sensitivity for the coincidence cross section.[9] It is clear from a comparison of the solid curve (resulting from the model introduced in Ref. 7 and identified as I in the table) with the dashed curve (resulting from the model introduced in Ref. 6 and identified as II in the table) that large differences in the theoretical cross sections exist, differences larger than the 15% found for the total cross section in Ref. 7. However, most of this difference arises from the different singlet interaction in the final state. This becomes clear from a comparison of the solid curve with the dot-dashed curve (resulting from the Barbour-Phillips ground state combined with the final-state parametrization I in the table). Thus, it would appear to

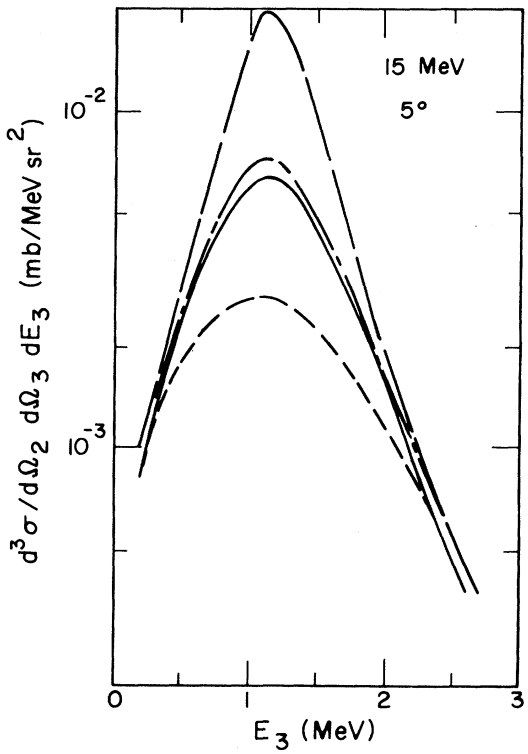

FIG. 7. Comparison of model results for the coincidence spectra at $E_\gamma = 15$ MeV and $\theta_2 = \theta_3 = 5°$. The solid curve describes the cross section for the Ref. 7 model in both the initial and final state; the long-dashed curve corresponds to the Ref. 6 model in both states; the dashed-dot curve corresponds to the Ref. 6 ground state and the Ref. 7 final-state parametrization; the short-dashed curve is similar to the solid curve, but with p-p singlet parameters in the continuum.

TABLE I. Model parametrizations.

Model	Ground state B_3 (MeV)	N_3 (fm^{-1})	C	$\bar{\alpha}$	$\bar{\beta}$	$\bar{\gamma}$	Continuum state λ (fm^{-3})	β (fm^{-1})	a (fm)	r_0 (fm)	
						I					
Ref. 7	7.72	0.307	1.000	4.93	1.92	0.133	0.3815	1.406	5.423	1.761	(trip.)
			0.335	3.38	0.913	0.0907	0.1323	1.130	−17.0	2.84	(sing.)
						II					
Ref. 6	7.71	0.372	1.000	6.15	2.89	0.353	0.391	1.418	5.397	1.747	(trip.)
			0.310	4.31	1.17	0.0821	0.148	1.150	−21.25	2.74	(sing.)
						III					
Ref. 7							0.3815	1.406	5.423	1.761	(trip.)
							0.1534	1.223	−7.823	2.794	(sing.)

be almost as difficult to determine significant differences in the two ground-state wave functions from the coincidence experiment as it would be from the total cross section measurement. A further complication can be noted by examining the short-dashed curve (resulting from the Barbour-Phillips ground state and the continuum parameters labeled III in the table—a singlet in-

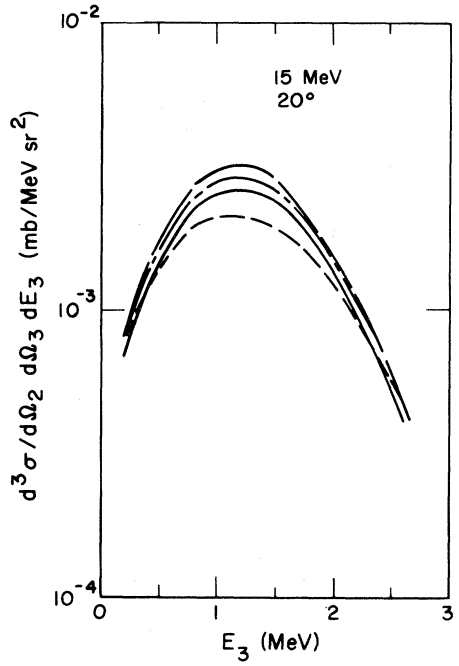

FIG. 8. Comparison of model results for the coincidence spectra at $E_\gamma = 15$ MeV and $\theta_2 = \theta_3 = 20°$. The solid curve describes the cross section for the Ref. 7 model in both the initial and final states; the long-dashed curve corresponds to the Ref. 6 model in both states; the dashed-dot curve corresponds to the Ref. 6 ground state and the Ref. 7 final-state parametrization; the short-dashed curve is similar to the solid curve, but with p-p singlet parameters in the continuum.

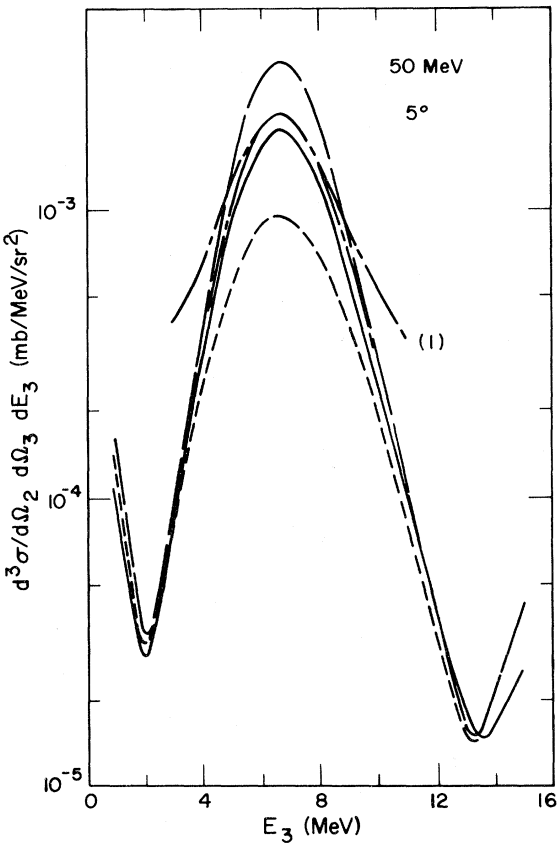

FIG. 9. Comparison of model results for the coincidence spectra at $E_\gamma = 50$ MeV and $\theta_2 = \theta_3 = 5°$. The solid curve describes the cross section for the Ref. 7 model in both the initial and final state; the long-dashed curve corresponds to the Ref. 6 model in both states; the dashed-dot curve corresponds to the Ref. 6 ground state and the Ref. 7 final-state parametrization; the short-dashed curve is similar to the solid curve, but with p-p singlet parameters in the continuum. The additional dashed-dot curve labeled (1) corresponds to the single-pair rescattering approximation to the dashed-dot curve.

teraction fitted to the modified p-p scattering length and effective range, but lacking the pure Coulomb scattering of the two protons). It is clear that the final-state interactions dominate the cross section, making it difficult to extract information about the ground-state wave function.

One might consider looking instead at a larger angle, such as the 20° opening angle shown in Fig. 8. One expects, from the results shown in Fig. 3, that the dominance of the cross section by the p-p rescattering will be lessened. That such is the case can be seen from a comparison of the same solid curve and long-dashed curve in this figure as we had in Fig. 7. The dot-dashed curve (again resulting from the Barbour-Phillips ground state, but with the continuum interaction identical to those used in obtaining the solid curve) coincides with the dashed curve in the tail of the cross section, where the details of the interaction producing the final-state rescattering effects become much less important. Near the peak of the cross section, this dot-dashed curve lies about halfway between the solid and dashed curves; this illustrates that, even in this geometry where none of the nucleons come out close together, about half the difference between models I and II in the table results from the ground state model and about half the difference from the different singlet interactions in the continuum. However, even here, a proper treatment of the p-p interaction would be necessary as one can ascertain by comparing the short-dashed curve with the first three.

One might also consider higher energy, such as 50 MeV. Here, near the peak of the cross section, one does find that the one-interacting-pair approximation is good. This can be seen by comparing the two dot-dashed curves in Fig. 9. However, the region of the spectrum where this approximation is valid is small. Thus one cannot escape the difficult task of including the differing singlet interactions ($V_{pp} \neq V_{np}^s$) separately in order to extract useful information about the ground state from the coincidence experiment. Restating this point: It would appear that one must allow for charge dependence in the N-N interaction. In addition, one would prefer the $^3\mathrm{H}(\gamma, 2n)p$ reaction in order to avoid the obvious Coulomb difficulties.

IV. CONCLUSIONS

The coincidence cross section has been shown to be much more sensitive to model dependence than the total cross section, as expected. However, much of the sensitivity is to the singlet final-state interaction and not to the ground state wave function; this is especially true when the geometry is such that two of the nucleons exit with little relative energy. At higher energies ($E_\gamma \sim 50$ MeV), it was found that the single-interacting-pair approximation is adequate near the peak in the spectrum where the relative energy of the pair is a minimum. Coulomb effects will likely make the theoretical analysis of the $^3\mathrm{He}(\gamma, 2p)n$ reaction difficult. Even in the less complex $^3\mathrm{H}(\gamma, 2n)p$ reaction, charge dependent forces ($V_{np}^s \neq V_{nn}$) will be required in order to make a meaningful analysis.

---

*Work performed under the auspices of the U. S. Energy Research and Development Administration.

[1]T. A. Griffy and R. J. Oakes, Phys. Rev. 135, B1161 (1964); Rev. Mod. Phys. 37, 402 (1965).

[2]A. Johansson, Phys. Rev. 136, B1030 (1964).

[3]B. F. Gibson and G. B. West, Nucl. Phys. B1, 349 (1967).

[4]D. R. Lehman, Phys. Rev. C 3, 1827 (1971).

[5]J. Matthews and H. Jeremie (private communication).

[6]I. M. Barbour and A. C. Phillips, Phys. Rev. C 1, 165 (1970).

[7]B. F. Gibson and D. R. Lehman, Phys. Rev. C 13, 477 (1976).

[8]The density of states defined in Eq. (8) contains a factor of 2 for identical particles; this compensates for the extra $\sqrt{2}$ appearing in the denominator of Eq. (6), where identical particles were ignored. It is clear that one can omit the factor of 2 in Eq. (8) and integrate over all of phase space [$\int d\Omega_2 d\Omega_3 = (4\pi)^2$] to obtain the correct total cross section, thus ignoring the question of identical particles in calculations such as those in Refs. 6 and 7.

[9]The models of Refs. 6 and 7 may be summarized as follows: For the ground state one assumes $\psi^s = \psi^{(1)} + \psi^{(2)} + \psi^{(3)}$, where $\psi^{(1)} = N_3[g_t(k)u_t(p) + g_s(k)u_s(p)]/(k^2 + \frac{3}{4}p^2 + K^2)$ and $K^2 = mB_3$. The spectator functions are $u_n(p) = C_n/(1 + \bar{\alpha}_n p^2 + \bar{\beta}_n p^4 + \bar{\gamma}_n p^6)$ and the form factors are $g_n(k) = (k^2 + \beta_n^2)^{-1}$. The separable potentials defining the continuum are the usual $v_n(k, k') = -(\lambda/m)g_n(k)g_n(k')$.